

On Minerals Associated with Ultrabasic Rocks, Found in the Vicinity of Common Boundaries of Shimane, Tottori, Okayama and Hiroshima Prefectures (VI)

— Lizardite and Clinochlore from the Wakamatsu Mine,
Tottori Prefecture —

Jun-ichi KITAHARA

Department of Geology and Mineralogy, Shimane University, Matsue, Japan

(Received November 29, 1969)

Abstract

Lizardite and clinochlore from the Wakamatsu mine, Tottori prefecture were investigated by means of X-ray, differential thermal and chemical analyses.

It was proved that the lizardite shows characteristic X-ray powder patterns as described in the paper.

Chlorite was identified by X-ray powder data, but the name clinochlore was determined by chemical composition.

The unit cell dimensions and the chemical compositions of the minerals are mentioned in the paper.

Introduction

Chrysotile, lizardite and antigorite compose the serpentine group minerals. The best classification of the minerals in the serpentine group is that of Whittaker and Zussman (1956) based on the X-ray diffraction result. Lizardite is generally known as a variety of serpentine minerals and the unit cell is single layered orthogonal ($\beta=90^\circ$). This mineral reported first by Midgley (1951) for a serpentine mineral from Kennack Cove, Lizard, Cornwall is white and platy.

It was identified by the writer that a bluish part of the ultrabasic rock distributed on the south level of Wakamatsu mine, Tottori prefecture is composed of lizardite by means of X-ray powder patterns, differential thermal analysis and chemical analysis.

Chlorites are a group of minerals with layered structure, which in many respects resemble the micas. It was investigated by X-ray powder method (McMurchy, 1934; Engelhardt, 1942; and others) that the structure of chlorites is one of regularly alternating talc-like and brucite-like sheets.

A clinochlore rock from the chūgiri level of Wakamatsu mine, Tottori prefecture was found by the writer as a xenolith in chromite body, and the clinochlore was studied by X-ray, differential thermal and chemical analyses.

Lizardite

X-Ray Powder Diffraction Patterns

The X-ray powder diffraction patterns of the lizardite from the above mentioned area

and heated specimen were taken by a Shimazu X-ray diffractometer. Ni-filtered copper radiation ($\text{Cu.K}\alpha$: 1.5418) was used under the following experimental conditions; 35 kV, time constant 1.25 seconds, scanning speed 1° per minute, chart speed 1 cm per minute, full scale 1,000 counts and slit 1 mm (divergent) - 0.2 mm (receiving). The typical diffractometer traces for the lizardite specimen and the changes observed in the X-ray powder patterns after successive heatings was summarized in Table 1.

The spacings and intensities of this specimen almost correspond to those of lizardite described by Whittaker and Zussman (1956). The reflections 202 at about 2.5 \AA and 204 at about 2.15 \AA , and the pair of reflections of 060 at about 1.54 \AA and 208 at about 1.51 \AA are available for the distinction of lizardite from antigorite and clinochrysotile. The strong line from antigorite at $d=2.52 \text{ \AA}$ may be confused with 202 of lizardite but it should be noted that in the latter varieties d_{202} has been observed about 2.51 \AA . The strong line at $d=1.563 \text{ \AA}$ in antigorite is important that it is not 060 and has no counterpart in chrysotile or lizardite patterns.

The moderately strong 060 ($d=1.537 \text{ \AA}$) and 208 ($d=1.506 \text{ \AA}$) in the specimen are not strictly equivalent to the strong pair at $d=1.535 \text{ \AA}$ and 1.503 \AA given by lizardite. The basal peaks (002, 004) of the specimen are strong as those of usual serpentine minerals, and particularly, the 011 peak is comparatively strong. These facts suggest that the lizardite is high in crystallinity. The lizardite (one-layer ortho-structure) shows a few weak reflections (130, 310).

Table 1. X-ray powder data for lizardite from the south level of Wakamatsu mine, Tottori pref.

hkl	Normal temp.		After 200°C		After 300°C		After 400°C	
	d	I	d	I	d	I	d	I
(001)							14.7	1
011	7.89	25						
002	7.38	100	7.43	83	7.49	44	7.36	47
020	4.63	12	4.61	12	4.65	7	4.61	8
022	3.93	8						
004	3.63	49	3.67	64	3.70	22	3.67	27
130	2.63	2	2.66	3	2.67	2		
202	2.508	36	2.511	20	2.514	15	2.51	25
203			2.350	3	2.347	1		
204	2.151	7	2.151	5	2.160	2	2.158	5
206					1.803	1		
310	1.720	2						
060	1.537	25	1.538	20	1.544	8	1.535	10
208	1.506	7	1.509	5	1.513	2	1.507	2

(001) : Chlorite-like

Unit cell of lizardite

$a^* = 0.1864$
 $b^* = 0.1084$
 $c^* = 0.0679$
 $\beta^* = 89.9^\circ$

$a = 5.364 \text{ \AA}$
 $b = 9.223 \text{ \AA}$
 $c = 14.711 \text{ \AA}$
 $\beta = 90^\circ$
 $V = 727.8 \text{ \AA}^3$

Table 1. (continued)

hkl	After 500°C	
	d	I
(001)	14.4	2
002	7.38	15
020*	5.14	1
022 ; 021*	3.91	2
101*	3.754	1
004	3.673	2
130*	2.784	2
202 ; 131*	2.610	8
112*	2.468	2
060	1.533	1

* : Olivine

Table 1. (continued)

hkl	After 600°C		After 700°C		After 800°C	
	d	I	d	I	d	I
(001)	14.2	1				
020	5.15	3	5.12	2	5.14	5
110			4.33	2	4.36	3
021	3.90	8	3.883	15	3.900	17
101	3.746	3	3.727	5	3.746	10
111	3.506	5	3.493	10	3.493	8
121 ; 221 ⁺			3.007	5	3.003	10
002	3.007	2	2.993	3		
310 ⁺			2.902	1	2.893	2
					2.871	1
130	2.775	8	2.771	17	2.771	22
131	2.521	12	2.514	25	2.514	39
112	2.468	10	2.461	41	2.461	29
041					2.347	3
210					2.320	3
122	2.275	7	2.267	12	2.270	24
140			2.245	7		
220, 211	2.165	2	2.163	7	2.163	7
330 ⁺			2.115	1		
132			2.096	1		
222	1.752	10	1.749	25	1.750	29
					1.672	3
					1.638	2
			1.623	2		
					1.615	5
			1.569	3		
			1.496	8	1.496	7

+ : Clinoenstatite

() : Chlorite-like

no mark : Olivine

Thermal Changes

On heating up to 400°C the lizardite still maintains well its original structure, and the basal peaks (002, 004) and the pair peaks (060, 208) decrease about 50% in intensity, the other peaks decrease moderately. The 011 peak found at normal temperature, diminishes at 200°C and chlorite-like 14.7 Å layer appears at 400°C after the partial dehydration. When heated at 500°C for one hour, the disruption of the original structure remaining the basal and 060 peaks almost completes, and forsterite peaks are observed and this is followed by disappearance of the lizardite at about 700°C. After heating at 600°C for one hour, the lizardite transforms to forsterite, remaining the reflection that diminishes from 14.7 Å down to 14.2 Å of chlorite-like layer. A part of the mineral is converted to an intermediate chloritic material with a spacing which remove from 14.7 Å at 400°C to 14.2 Å at 600°C as mentioned above. An amorphous state is distinctly presented at 500°C and followed by the appearance of forsterite pattern. Here the intensity of the low angle reflection (001) (chlorite-like layer) at 600°C is weaker than the one of 500°C, and then at 700°C the chlorite-like reflection is not observed. It may be considered that the formation of the chlorite-like 14 Å layer is contained appreciable amount of alumina and ferric oxide in the specimen, and it may also be recalled that chlorite-like layer persisted after the partial dehydration of magnesia chlorite. After heating at 700°C for one hour, forsterite patterns with slight clino-enstatite reflection from the mineral are remarkably developed before or after the lizardite reflections completely disappeared.

Serpentines transform to forsterite in the same general way as do magnesian chlorites. Although the final transformation appears to be closely similar for all structural varieties of serpentines, the transitional stage appears to depend on whether the initial minerals have a two-layer or a one-layer type of structure. It is said that the two-layer serpentines behave similarly to the two-layer alumina silicate, giving a transitional product with a nearly constant 14.5 Å spacing, while the one-layer serpentines generally give a transitional product with a spacing which diminishes from about 14 Å down to 10 Å.

The transformation of pure lizardite (magnesian serpentine) to forsterite is as the following relation.



The unit cell relations, $2a_{\text{S}(\text{Serp.})} \simeq b_{\text{F}(\text{Fo.})}$ and $2s \simeq 3c_{\text{F}}$, show that four cells in one layer of serpentine transform to 3 cells in one layer of forsterite.

It is possible to determine the composition from the X-ray diffraction powder data. The molecular fraction (x) of the olivine generated at 800°C from the specimen is calculated as follows :

$$x = 15.8113 / \sqrt{3.0358 - d(130)} - 7.2250 \quad (\text{Fisher and Medaris, 1969}) \\ = 0.911,$$

$$\text{Fo (mole \%)} = 91.1.$$

$$\text{Fo (mole \%)} = 4233.91 - 1494.39 \times d(130) \quad (\text{Yoder and Sahama, 1957}) = 90.9.$$

The lattice parameter and the unit-cell volume of the olivine ($\text{Fo}_{90.9}$) generated at 800°C are listed as follows :

$$a=4.760 \text{ \AA}, b=10.220 \text{ \AA}, c=5.991 \text{ \AA}, V=291.4 \text{ \AA}^3.$$

Differential Thermal Analysis

The differential thermal analysis curve (Fig. 1) for the mineral was obtained under the heating rate of 10° per minute and chart speed of 4 mm per minute. The differential curve consists of their principal peaks : (1) an endothermic peak at about 104°C , appearing small endothermic reaction-like forms at 222°C , 402°C and 661°C , (2) a relatively broad but well-marked endothermic peak at 664°C , starting at about 614°C and finishing at about 700°C , and (3) a strong, sharp exothermic peak at 795°C , starting at about 780°C and finishing at 810°C . The low temperature endothermic peak is mostly caused by the removal of absorbed water. The high temperature endothermic reaction between about 600°C and 700°C , which is due to dehydration of constitutional water but it is not so much investigated as compared with those of chrysotile and antigorite. The pre-temperature region of this endothermic reaction corresponds to the formational stage of chlorite-like material. The endothermic peak agrees to the expulsion of structural water as mentioned above or the complete decomposition of its structure. Between 700°C and 780°C , no thermal reaction can be recognized on the curve, so it is indicated that the stage is amorphous state before the formation of forsterite. The sharp exothermic peak seems to be related to the formation of forsterite and/or enstatite between 700°C and 800°C , but in the specimen heated at 500°C , olivine is slightly appeared on the X-ray powder pattern.

Chemical Analysis

The lizardite specimen was chemically analyzed by the writer. The chemical composition and atomic ratios calculated on the basis of $(\text{O}, \text{OH})=9$ are shown in Table 2.

In the general formula of natural serpentine $X_6Y_4O_{10}(\text{OH})_6$, X represents the possibility for the substitution of the ions Mg^{2+} , Fe^{2+} , Fe^{3+} , Co^{2+} , Ni^{2+} , Mn^{2+} , Cr^{3+} , Cu^{2+} , Al^{3+} ,

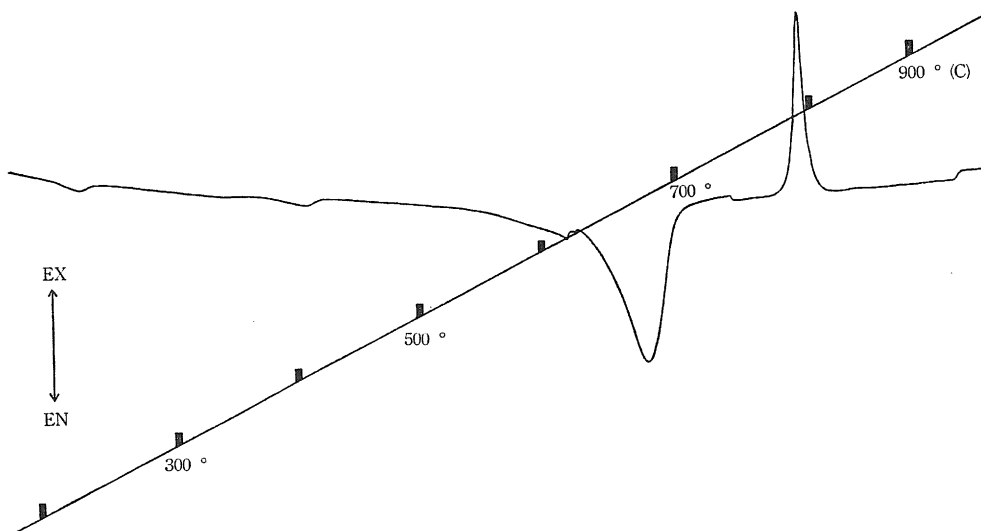


Fig. 1. Differential thermal curve for the lizardite from the Wakamatsu mine, Tottori pref.

Table 2. Lizardite from the south level of Wakamatsu mine, Tottori pref.

	Wt%	Mols		Atom. ratios	(O, OH)=9.00
SiO ₂	38.52	641	Si	641	1.810
TiO ₂	0.01	0.1	Ti	0.1	0.0003
Al ₂ O ₃	2.33	23	Al	46	0.130
Fe ₂ O ₃	3.64	23	Fe ³	46	0.130
FeO	1.95	27	Fe ²	27	0.076
NiO	0.06	0.8	Ni	0.8	0.002
MnO	0.07	1	Mn	1	0.003
MgO	38.36	959	Mg	959	2.708
CaO	0.13	2	Ca	2	0.006
Na ₂ O	0.07	1	Na	2	0.006
K ₂ O	0.02	0.2	K	0.4	0.001
H ₂ O ₊	13.97	776	H ₊	1552	OH 4.383
H ₂ O ₋	0.62		O	3187.2	O 4.617
	99.75				

Tetrahedral ions		Octahedral ions	
Si ⁴⁺	1.810	Al ³⁺	-
Al ³⁺	0.130	Ti ⁴⁺	0
	1.940	Fe ³⁺	0.130
		Fe ²⁺	0.076
Anions		Ni ²⁺	0.002
O ²⁻	4.617	Mn ²⁺	0.003
(OH) ⁻	4.383	Mg ²⁺	2.708
	9.000	Ca ²⁺	0.006
		Na ⁺	0.006
		K ⁺	0.001
Σ Charges on anions	13.618		
Σ Charges on cations	13.617		2.932

(Analyst: J. Kitahara)

and Ti⁴⁺ in octahedral coordination; Y represents Si⁴⁺, Al³⁺, and Fe³⁺ in tetrahedral coordination and OH represents (OH)⁻, Cl⁻, and F⁻.

A ratio of Fe₂O₃ to FeO for the lizardite is larger than that of antigorite or chrysotile. If the mineral formula is calculated on the assumption of 14 negative charges, the average sum of octahedral cations is 2,932, but involves excess (4.383) of hydroxyl. The sum of tetrahedral ions for the lizardite is 1,940, and low than 2.00 (Table 2). The lizardite have lower ratio (10.7) of (Fe²⁺+Mg²⁺) to (Fe³⁺+Al³⁺) than that of normal chrysotile (Fig. 2). The anion charges of the lizardite are 13.618 and those of cations are 13.617 (Table 2). Those values are almost equal, so it shows that the chemical analysis is correct.

Occurrence

The principal occurrences of serpentine minerals are those in which they are derived

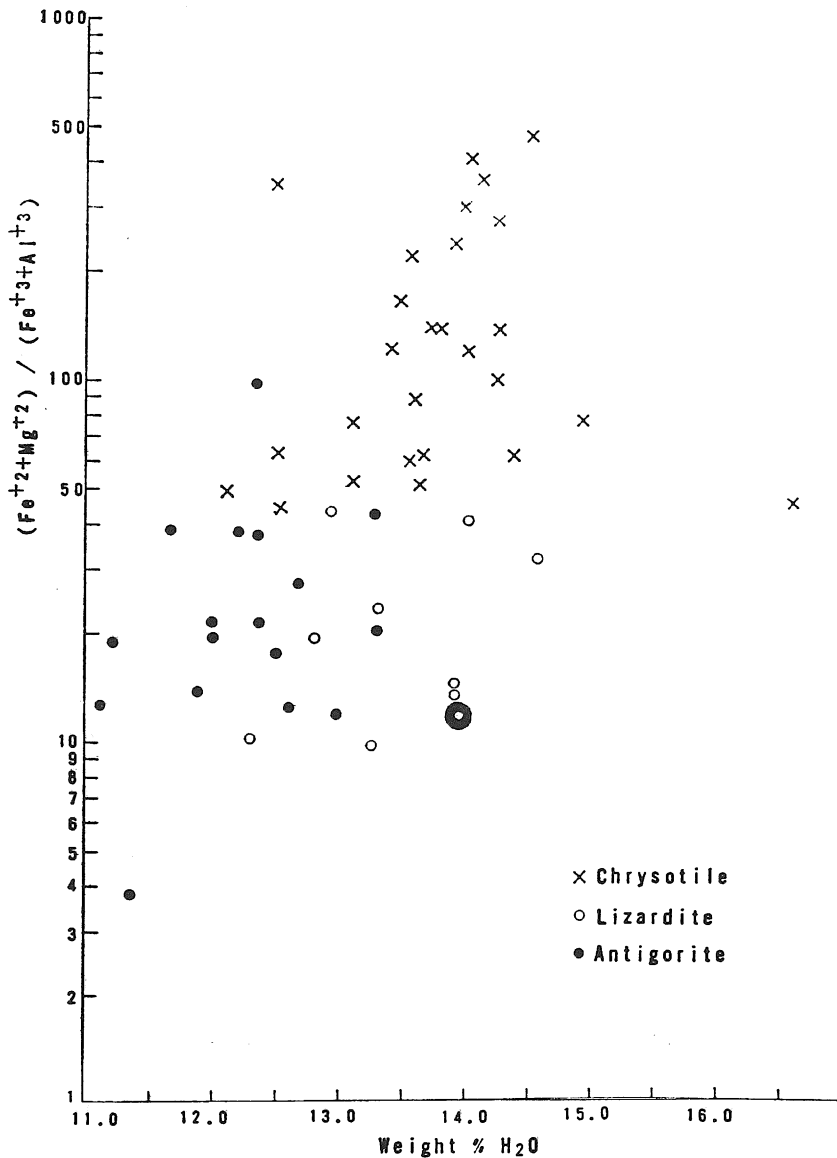


Fig. 2. $(\text{Fe}^{2+} + \text{Mg}^{2+}) / (\text{Fe}^{3+} + \text{Al}^{3+})$ versus weight percent H_2O for serpentines. (After Page.) Great open circle represents the chemical composition of lizardite from the Wakamatsu mine, Tottori pref.

from ultrabasic rocks. The processes which serpentinization takes place in such rocks as dunites, pyroxenites and peridotites have been the subject of much discussion. The formation of serpentines by the action of water on forsterite can occur only below 400°C . Bowen and Tuttle suggest that the olivine and pyroxene are intruded in the crystalline state without water, and are subsequently serpentinized below 500°C by water vapour acquired through contact with wet rocks. If the three varieties have no essential chemical difference, it could also be inferred that the formation of each polymorph in nature is favoured by particular environmental conditions: Lizardite (\pm

chrysotile) serpentinite generally occurs in higher-grade static metamorphism. In lower-grade static metamorphism, massive ultrabasic rocks consist predominantly of lizardite, whereas shearing produces preferentially chrysotile. Antigorite originates in a higher dynamometamorphic environment. The area is predominantly composed of serpentized harzburgite, but it is considered that a small part of dunite only in the ultrabasic rock, was hydrothermally autometamorphosed to lizardite.

Clinochlore

X-Ray Powder Data

The X-ray diffraction patterns of the clinochlore from the chūgiri level of Wakamatsu mine, Tottori prefecture were taken by Shimazu X-ray equipment under the above mentioned same experimental conditions. The X-ray powder patterns and data for normal and successive heating specimens are as shown in Fig. 3 and Table 3. The clinochlore rich in magnesia and alumina gives moderately weak reflection for 001 and 003 net planes and comparatively strong peak for 002 and 004 ones. The identification by X-ray analysis for the various forms of chlorite is very difficult unless chemical and optical data are available. The lattice constants of the specimen computed from the reciprocal lattice are as the following description :

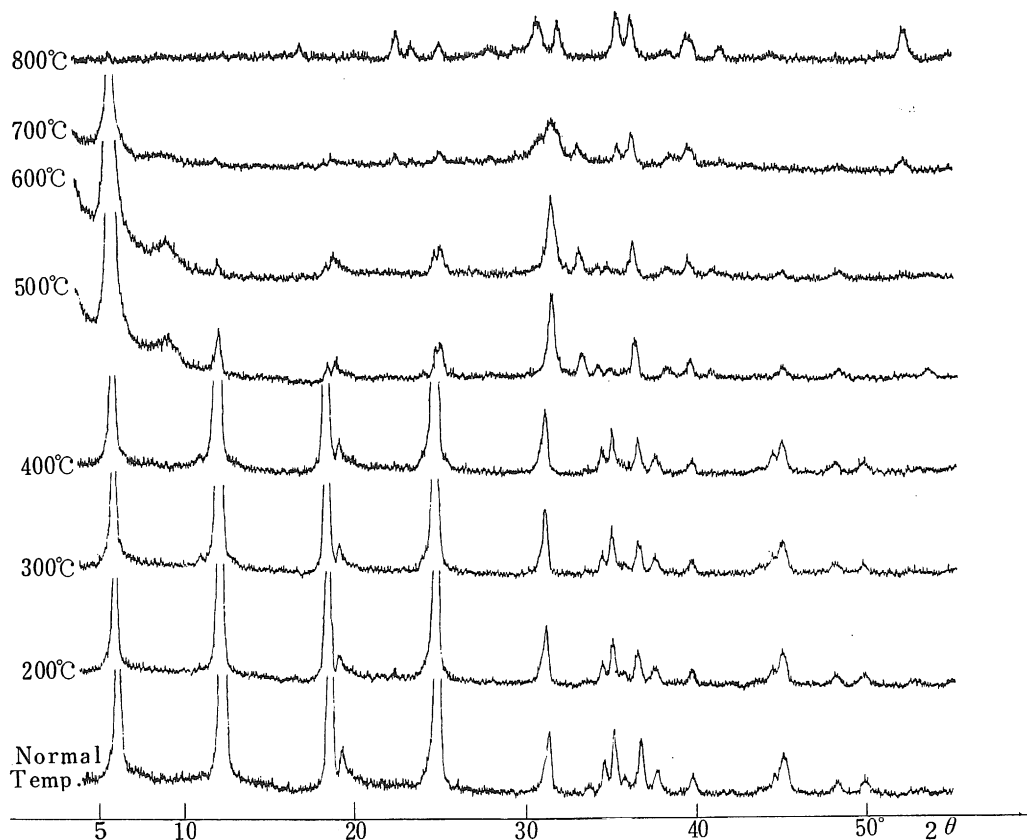


Fig. 3. X-ray powder diffraction patterns for clinochlore and its heated specimens.

$$\begin{aligned}
 Q_{004} &= 0.0788, Q_{201} = 0.1543, Q_{204} = 0.2475, Q_{060} = 0.4232. \\
 a^* &= 0.0701, b^* = 0.1084, c^* = 0.1890, \beta^* = 83^\circ 2'. \\
 a &= 5.330 \text{ \AA}, b = 9.223 \text{ \AA}, c = 14.353 \text{ \AA}, \beta = 96^\circ 58', \\
 d_{100} &= 5.291 \text{ \AA}, V = 700.4 \text{ \AA}^3.
 \end{aligned}$$

Thermal Changes

Each of the fine powdered specimens was heated in an electric furnace, and kept at successive temperatures from 200°C to 800°C at intervals of 100°C. After cooling, the diffractometer traces of each of the heated specimens were obtained with Shimazu X-ray equipment as described above.

In the course of the transformation from clinochlore to olivine, silica and water are expelled from the structure, but the role of aluminum is not understood for clinochlore, where the Al_2O_3 content is greater, the formation of olivine is impeded. When the clinochlore specimen is heated in electric furnace, olivine appears at 700°C on the X-ray diffraction pattern, but chlorite structure is still remained. The structure of clinochlore is almost decomposed, remaining slightly 001 reflection at 800°C. Thermal data are considerably influenced by the state of substitution of the specimen, and by the precise chemical composition, particularly iron content. For chlorite the 14 Å spacing is not generally changed on moderately heating to about 700°C. The specimen have a

Table 3. X-ray powder data for clinochlore from the chūgiri level of Wakamatsu mine, Tottori pref.

hkl	Normal temp.		After 200°C		After 400°C	
	d	I	d	I	d	I
001	14.3	42	14.6	30	14.4	40
002	7.16	83	7.21	61	7.16	75
003	4.75	44	4.78	42	4.77	47
020	4.59	5	4.64	5	4.61	3
004	3.56	53	3.58	60	3.57	51
005	2.84	15	2.86	15	2.86	15
13 $\bar{1}$, 10 $\bar{5}$	2.65	2				
131, 20 $\bar{2}$	2.58	5	2.58	3	2.58	3
13 $\bar{2}$, 201	2.54	12	2.54	6	2.54	7
132, 20 $\bar{3}$	2.44	8	2.45	5	2.44	6
13 $\bar{3}$, 202	2.38	4	2.39	3	2.38	4
133, 20 $\bar{4}$	2.26	3	2.28	2	2.26	3
007	2.029	2	2.036	2	2.034	4
13 $\bar{5}$, 204	2.010	13	1.993	7	2.009	8
135, 20 $\bar{6}$	1.887	3	1.891	2	1.889	3
13 $\bar{6}$, 205	1.827	4	1.827	2	1.827	2
137, 20 $\bar{8}$	1.569	9	1.572	9	1.569	8
060, 33 $\bar{1}$	1.537	8	1.538	5	1.538	5
062, 331	1.503	3	1.504	2	1.503	2
0.0.10			1.424	1	1.425	2
208	1.400	4	1.399	8	1.399	7

Table 3. (continued)

hkl	After 500°C		After 600°C	
	d	I	d	I
001	14.2	100	14.2	79
010	9.45	3	9.56	4
002	7.19	9	7.21	2
003	4.78	2	4.76	5
020	4.64	2	4.67	6
004	3.56	7		
005	2.82	26	2.81	24
13 $\bar{1}$, 10 $\bar{5}$	2.67	6	2.68	5
131, 20 $\bar{2}$	2.61	2	2.60	1
13 $\bar{2}$, 201	2.56	2	2.56	1
132, 20 $\bar{3}$	2.45	8	2.46	6
13 $\bar{3}$, 202	2.33	2	2.34	2
133, 20 $\bar{1}$	2.26	4	2.26	2
			2.19	2
13 $\bar{5}$, 204	2.008	2	2.006	2
135, 20 $\bar{6}$	1.882	1	1.886	2
136, 20 $\bar{7}$	1.712	2		
060, 33 $\bar{1}$	1.546	6	1.553	5
062, 331	1.514	3		
208	1.387	3		

basal spacing of approximately 14.3 Å–14.6 Å, and is stable when heated to 500°C.

The mole percent of forsterite generated at 800°C from the clinochlore is as follows :

$$\begin{aligned} \text{Fo (mole \%)} &= 4233.91 - 1494.59 \times d(130) \quad (\text{Yoder and Sahama, 1957}) \\ &= 4233.91 - 1494.59 \times 2.776 \\ &= 85.0. \end{aligned}$$

$$x = 15.8113 \sqrt{3.0358 - d(130)} - 7.2250 \quad (\text{Fisher and Medaris, 1969})$$

$$= 0.839,$$

where

x : mole fraction of forsterite

$$\text{Fo (mole \%)} = 83.9.$$

The mole percent of above mentioned sample that derived from d(112) (Jahanbaggio, 1969) is 85.0.

The unit cell dimension of the forsterite (85.0 mole %) is as follows : a=4.858 Å, b=10.256 Å, c=6.012 Å, V=294.0 Å³.

Differential Thermal Analysis

The fine-grained clinochlore shows an endothermic peak at 110°C, to expulsion of adsorbed water. That position of peak affected by composition is proved by curve from the clinochlore, which is the first large endothermic peak at 655°C. The temperature of the second endothermic peak is related to the amount of silicon in the tetrahedral sheet ; the higher the silicon content, the higher the temperature of this peak. Thus the

Table 3. (continued)

hkl	After 700°C		After 800°C	
	d	I	d	I
001	14.2	41	14.2	1
002	7.19	1		
020*	5.12	1	5.14	1
021*	3.90	2	3.883	4
101*			2.738	2
004	3.513	2		
111*			3.506	3
220 ⁺			3.158	1
310 ⁺	2.862	1	2.875	10
005	2.809	19		
130*			2.775	5
	2.682	2		
131*	2.514	2	2.514	11
112*	2.461	9	2.461	11
	2.323	2		
122*	2.267	5	2.270	3
140*			2.253	3
220*, 211*			2.163	3
222*	1.749	3	1.749	7
			1.672	1
	1.615	1		
137, 20 $\bar{8}$	1.559	1		
060, 33 $\bar{1}$	1.553	2		
			1.492	1
* : Olivine			1.475	1
+ : Clinoenstatite			1.392	1

clinochlore specimen decomposes at temperature of 805°C, and is followed by a small exothermic reaction.

The exothermic peak occurs at 817°C, and the peak is related to the formation of forsterite and clinoenstatite.

Chemical Analysis

The specimen is readily attacked by hydrochloric acid leaving behind a colloidal silica. In the case of a magnesian chlorite, it has been suggested that aluminian ions in tetrahedral coordination are less readily removed than those of octahedral sites.

The pure specimen was analyzed by the writer, and the atomic ratios were calculated by means of a computer.

The result is shown in Table 4. Tetrahedral and octahedral ions are denoted in Table 4, based on 4 of tetrahedral ions.

In chlorites a wide range of substitutions occur in talc and brucite layers, silicon being replaced by aluminum within the range $[\text{Si}_{3.5}\text{Al}_{0.5} - \text{Si}_2\text{Al}_2]^t$. A first subdivision is made between chlorites with more than 4 percent Fe_2O_3 and those with less, and

Table 4. Clinocllore from the chūgiri level of Wakamatsu mine, Tottori pref.

	Wt%	Mols	Atom. ratios		Ditto when(O, OH)=18
SiO ₂	32.61	544	Si	544	3.070
TiO ₂	0.02	.3	Ti	.3	0.002
Al ₂ O ₃	19.77	194	Al	388	2.190
Fe ₂ O ₃	1.73	11	Fe ³	22	0.124
FeO	1.15	16	Fe ²	16	0.090
NiO	0.25	3	Ni	3	0.017
MnO	0.01	.1	Mn	.1	0.001
MgO	32.76	819	Mg	819	4.622
CaO	0.03	.5	Ca	.5	0.003
Na ₂ O	0.03	.5	Na	1	0.006
K ₂ O	0.02	.2	K	.4	0.002
H ₂ O ⁺	11.61	645	H	1290	OH 7.281
H ₂ O ⁻	0.08				O 10.719
	100.07				

(Analyst: J. Kitahara)

Table 4. (continued)

Tetrahedral ions		Octahedral ions	
Si	3.070	Al	1.260
Al	0.930	Ti	0.002
	4.000	Fe ³	0.124
		Fe ²	0.090
		Ni	0.017
		Mn	0.001
		Mg	4.622
		Ca	0.003
		Na	0.006
		K	0.002
			6.127
Clinocllore (composition range)			
(Al _{1.35-.70} Fe ³ _{.00-.80} Fe ² _{.00-.80} Mg _{3.65-5.10})			
(R ³ _{1.45-.00} R ² _{4.45-5.10})(Si _{2.76-3.10} Al _{1.24-.90})O ₁₀ (OH) ₈ with Fe ² /R ² <0.25.			
R ³ =1.384, R ² =4.733, Si=3.070, Al=0.930, Fe ² /R ² =0.019 (clinocllore specimen)			

these are termed oxidized and unoxidized respectively. Unoxidized chlorites are the most common and for these divisions are drawn according to Si content. Chlorites were produced from composition with more than 0.50 Al per formula unit at temperatures above 500°C. Septechlorites were produced for all composition from Mg₃Si₂O₅(OH)₄ (serpentine) up to (Mg₂Al)(SiAl)O₃(OH)₄ at temperatures below 500°C. The number of silicon atoms per formula unit of the specimen is 3.07 out of a maximum of 4. Tetrahedral coordination is 0.93 atoms of Al, and octahedral coordination is 1.26 atoms of Al. Chlorites are described by three suitable parameters: ferric iron, silicon, and total iron. The idealized composition of a pure magnesian chlorite should be

$Mg_3Si_4O_{10}(OH)_2$, $Mg_3(OH)_6$. In it Mg can be replaced by Fe^{2+} , Fe^{3+} , Al, Cr^{3+} , Ni, or Mn, Al also replacing Si in the tetrahedral sites. The general formula of chlorite should be written as $(Mg, Fe, Al, Cr, Ni, Mn)_3(Si, Al)_4O_{10}(OH)_2$, $(Mg, Fe, Mn)_3(OH)_6$. The chemical composition range of clinochlore is shown in Table 4. The clinochlore composition $(Mg_{1.6}Fe_{0.2}Al_{1.3})(Si_{3.1}Al_{0.9})O_{10}(OH)_8$ (Fig. 4) was calculated from the chemical analysis and confirmed by the position and intensity of the 001 reflection on the diffractogram. The clinochlore composition is limited in the range as shown in the table.

Occurrence

Chlorites are common constituents of igneous rock in which they have generally been derived by the hydrothermal alteration of primary ferromagnesian minerals. The composition of chlorite is often related to that of original igneous rocks, and clinochlore (aluminum-rich chlorite) is commonly found as replacement of aluminum rich enstatite. The formation of chlorites, during the regional metamorphism of ultrabasic rocks is not common, but has been described from a number of localities.

The nickel-containing clinochlore specimen in the region is related to ultrabasic rocks, which have undergone hydrothermal alteration of enstatite rich xenolith in a chromite body. Here the earlier deuteritic chloritization of primary enstatite has been followed by

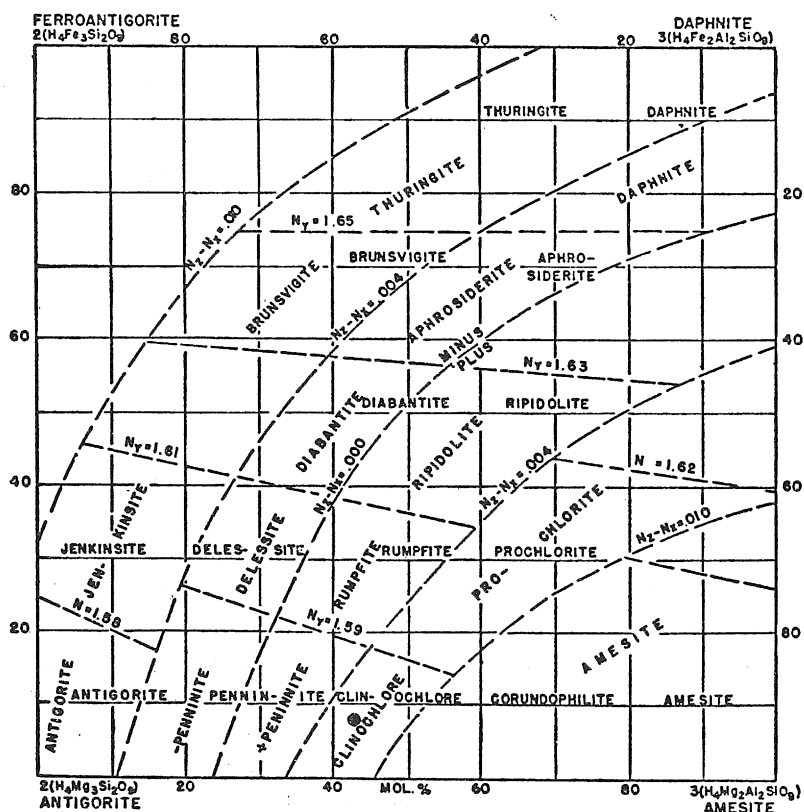


Fig. 4. Chemical and optical classifications of chlorite. (After Winchell.) Dot represents the analysis of clinochlore from the Wakamatsu mine, Tottori pref.

more extensive hydrothermal action. The hydrothermally formed chlorite differs from the deuteric chlorite in being fine-grained and colourless. The clinocllore is the last mineral of the hydrothermal alteration sequence, and in the most advanced stage of the alteration almost completely replaced the earlier formed talc. Thus, it appears that the deuteric hydrothermal alteration of pre-existing rocks in the region resulted in the formation of chlorite and serpentine in large amounts as described above.

Acknowledgements

The writer wishes to express his cordial thanks to the head of Wakamatsu mine, Nippon Chrome Kōgyō K. K., Mr. Thuneo Nozaka, the members of the staff of the mine including Messrs Kizō Kimura and Kazuo Kinutani for the writer's survey of the mine. The expenditure of this investigations has been partly defrayed by the Scientific Researches of the Ministry of Education, to which the writer wishes to express his thanks.

References

- Bowen, N. L. and Tuttle, O. F., 1949. The system $MgO-SiO_2-H_2O$. *Bull. Geol. Soc. Amer.*, **60**, p. 639.
- Brown, G., 1961. The X-ray identification and crystal structures of clay minerals. *Min. Society, London*.
- Deer, W. A., Howie, R. A. and Zussman, J., 1963. *Rock forming minerals*. **3**, Longmans.
- Fisher, G. W. and Medaris, L. G., Jr., 1969. Cell dimensions and X-ray determinative curve for synthetic magnesium-ferric olivines. *Amer. Min.*, **54**, p. 741.
- Foster, M. D., 1962. Interpretation of the composition and a classification of the chlorites. *U. S. Geol. Survey, Prof. Paper*, **414-A**, 1.
- Gillery, F. H., 1959. X-ray studies of synthetic Mg-Al serpentines and chlorites. *Amer. Min.*, **44**, p. 143.
- Hey, M. H., 1954. A new review of the chlorites. *Min. Mag.*, **30**, p. 277.
- Jahanbagloo, C., 1969. X-ray diffraction study of olivine solid solutions. *Amer. Min.*, **54**, p. 246.
- Nelson, B. W. and Roy, R., 1958. Synthesis of the chlorites and their structural and chemical constitution. *Amer. Min.*, **43**, p. 707.
- Page, N. J., 1968. Chemical differences among the serpentine "polymorphs". *Amer. Min.*, **53**, p. 201.
- Shirozu, H., 1958. X-ray powder patterns and cell dimensions of some chlorite in Japan, with a note on their interference colours. *Min. Journ. Japan*, **2**, p. 209.
- Tomisaka, T. and Kato, T., 1963. A study on the polymorphs of serpentine minerals. *Min. Journ. Japan*, **6**, p. 209.
- Whittaker, E. J. W. and Zussman, J., 1956. The characterization of serpentine minerals by X-ray diffraction. *Min. Mag.*, **31**, p. 106.
- , 1958. The characterization of serpentine minerals. *Amer. Min.*, **43**, p. 917.
- Yoder, H. S., Jr. and Sahama, T. G., 1957. Olivine X-ray determinative curve. *Amer. Min.*, **42**, p. 475.